



OPEN

Diploid aposporous sunflower forms triploid BIII progeny displaying increased apospory levels and non-random genetic mutations

Silvina Pessino^{1,2,5}, Graciela Nestares^{1,2,5}, Marta B. Bianchi^{1,3}, Iara Kazaroff¹, Lucía Amato^{1,2}, Marika Bocchini⁴, Gianpiero Marconi⁴, Emidio Albertini⁴ & Ana C. Ochogavia^{1,2}✉

Apomixis (asexual reproduction via seeds) has the potential to revolutionize sunflower breeding. In previous studies, we identified a diploid sunflower line (Rf975) that naturally exhibits extra gametophytes resembling aposporous apomictic embryo sacs (AES). Here, we investigated the nature (reduced vs. unreduced) and viability of these AES-like gametophytes by examining the formation of triploid (3x) BIII hybrids ($2n + n$) in the progeny of Rf975. Flow cytometry analysis of immature seeds revealed that, on average, 42.8% of self-pollinated Rf975 progeny were triploids, although only 36.6% of them reached maturity. Cytoembryological analysis showed that 100% of triploids exhibited some degree of apospory, with an average expressivity of 61.9%. Abnormal pollen grains and limited viable seeds were also noted. A segregant F_2 progeny, comprising diploid and triploid individuals, was generated by crossing Rf975 with HA89, a genetically divergent sexual diploid. SNP-based progeny tests discarded that diploid Rf975 forms clonal matroclinal progeny at levels greater than 18%. Furthermore, specific non-random genetic and DNA methylation changes were detected in the F_2 triploids compared to F_2 diploids and parental plants, highlighting recurrent (epi)genetic alterations occurring during triploidization. This research could contribute to the future implementation of apomixis-based strategies in sunflower breeding.

Keywords Apospory, Cytoembryology, Flow cytometry, *Helianthus annuus* L., Molecular markers, Plant breeding, Polyploidy

Sunflower (*Helianthus annuus* L.) is a major oilseed crop, widely cultivated for the production of edible oils and biodiesel^{1,2}. This drought-resistant species thrives in a variety of soil conditions³. However, its expansion into regions with poor soil quality and increased agroecological stress has led to significant yield reductions, posing a challenge for plant breeders^{3–5}. To address this, the development of new commercial hybrids with enhanced tolerance to adverse environmental conditions, as well as improved quality and yield, is essential for boosting sunflower productivity and competitiveness. There is a pressing need to develop stabilized cultivars that not only exhibit high adaptability and superior seed quality but also offer more efficient and cost-effective production than current varieties³.

Following maize, sunflower ranks as the second most important crop for hybrid breeding⁶. The development of modern sunflower seed production systems can be attributed to two key events: the discovery of cytoplasmic male sterility by Leclercq in France⁷ and the identification of fertility-restoring genes by Kinman in the USA⁸. Today, sunflower is predominantly cultivated as a single-cross hybrid. The hybrid seed production system relies

¹Facultad de Ciencias Agrarias, Universidad Nacional de Rosario (FCA-UNR), Campo Exp. Villarino, Zavalla, Santa Fe, Argentina. ²Instituto de Investigaciones en Ciencias Agrarias de Rosario (IICAR-CONICET-UNR), Campo Exp. Villarino, Zavalla, Santa Fe, Argentina. ³Consejo de Investigaciones de la Universidad Nacional de Rosario (CIUNR), Rosario, Argentina. ⁴Dipartimento di Scienze Agrarie, Alimentari ed Ambientali, Università degli Studi di Perugia, Perugia, Italy. ⁵Silvina Pessino and Graciela Nestares contributed equally to this work. ✉email: ana.ochogavia@conicet.gov.ar

on the development and maintenance of four parental lines: the male-sterile line (A), the maintainer line (B), the fertility-restorer line (R), and the commercial hybrid (A × R). Key traits of these parental lines—such as female productivity, pollen production in restorer lines, and flowering synchronization—are crucial factors influencing seed productivity⁹. Additionally, because F_1 hybrid vigour diminishes in subsequent generations due to segregation, seed producers must continually generate new seeds through sexual crosses between the parental lines, which is a costly process.

Introducing apomixis into sunflower breeding could significantly accelerate the development of improved hybrids. Incorporating apomixis into the breeding schemes of sexual plants eliminate the need for recurrent hybrid seed production through sexual crosses and shorten the time required to release new elite cultivars, as parental lines would no longer need to be homozygous^{10–13}. This reproductive mode bypasses meiosis to form unreduced female gametophytes and produces embryos with maternal genotypes through parthenogenesis (i.e., without fertilization), while also generating viable, reduced pollen, which is often necessary to form the endosperm by pseudogamy (i.e., fertilization of the central cell)¹⁴. In apomixis-based breeding programs, sexual mother plants are crossed with apomictic pollen donors to produce variable F_1 hybrids. Some of these hybrids are capable of clonal reproduction for multiple generations, as they inherit the apomixis trait from the father¹⁵. These hybrids can generate viable offspring even when derived from genetically distant parents, thus fostering crop diversification and enabling more efficient use of available germplasm for further improvement¹⁵.

In 2022, our research group made a significant breakthrough in introducing apomixis into sunflower breeding with the identification of two diploid fertility restorer lines (Rf974 and Rf975), which naturally form moderate levels of aposporous-like embryo sacs¹⁶. Previously, an apospory-like phenotype had been reported in male-sterile sunflower lines pollinated by wild *Helianthus* species¹⁷. Aposporous apomixis is characterized by the formation of non-reduced female gametophytes from the nucellar and integumental cells surrounding the meiotic gametic line (apospory), followed by parthenogenesis and successful endosperm formation after pseudogamy, even in the absence of the typical maternal-to-paternal genomic balance¹⁸. Like other mechanisms of agamospermy, this trait is genetically determined and is often associated with polyploidy and/or hybridity¹⁸.

In apomictic species, the formation of triploid (3x) hybrids from the fertilization of unreduced female gametes has been well-documented. Non-reduced egg cells can generate via apomeiosis and then be fertilized, resulting in triploid (2n + n) embryos and offspring, often referred to as BIII hybrids in the literature¹⁹. These hybrids, likely produced through an incomplete coupling of apospory and parthenogenesis, typically exhibit higher ploidy and increased expression of apomixis compared to diploids^{20–22}. It has been suggested that apospory is linked to extended egg cell receptivity, which reduces the frequency of parthenogenetically formed embryos and increases BIII seed formation^{21,23}. Notably, apospory and parthenogenesis are believed to be controlled by distinct genetic mechanisms, and the coordination of these processes remains unclear^{23–25}. Although BIII hybrids are typically formed at low frequencies, they are evolutionarily significant. These embryos differ in ploidy from both the maternal plant and their sexually produced siblings, and they contribute to subsequent tetraploidization through the establishment of a female triploid bridge²⁶.

This study aimed to investigate the presence of aposporous embryo sacs in the sunflower line Rf975 and assess their viability, specifically by exploring the formation of triploid (3x, BIII) hybrids (2n + n) via apospory followed by fertilization. Additionally, we examined the possible generation of clonal maternal progeny in Rf975. Our initial hypothesis was that the non-reduced embryo sacs detected by Menéndez et al.¹⁶ could occasionally be fertilized to form viable triploid progeny and/or could generate clonal progeny through apomixis. The occurrence of aposporous embryo sacs (AES) was analysed using DIC cytoembryology, the formation of triploid offspring was studied through flow cytometry on immature embryos and progeny leaves, the 2n:1n maternal:paternal origin of the triploid hybrids was inferred from cytoembryological features (i.e., megagametophyte and pollen development analysis), and the production of clonal maternal progeny was assessed through molecular progeny tests involving crosses between Rf975 and the genetically divergent line HA89.

Results

Rf975 forms BIII (2n + n) hybrid embryos and shows a reduced seed number

The number of young fruits (capitulum stage R6) and mature seeds (capitulum stage R8) was determined using image analysis²⁷ in the diploid, aposporous Rf975 genotype, and compared with the diploid sexual control line HA89 (Fig. 1). At R6, the estimated number of ovaries per capitulum was similar for both genotypes ($1,503 \pm 107$ and $1,563 \pm 109$, respectively, $p = 0.305$) (Fig. 1, A-B, E-F). However, at R8, Rf975 produced significantly fewer viable seeds than HA89 (709 ± 76 vs. $1,534 \pm 147$, respectively; $p = 6.6e^{-7}$) (Fig. 1, C-D, G-H). These numbers show that, in Rf975, 794 (1,503–709) of the initial 1,503 ovaries counted at R6 aborted between R6 and R8, representing 52.8%. Flow cytometry analysis of R6 embryos excised from the capitula revealed a high proportion of triploids in the Rf975 genotype (42.8% of the Rf975 R6 embryos were triploids; 95% confidence interval [CI]: 26.7–60.4%; $n = 35$; Fig. 1, I). The rest of the excised embryos were diploid (57.2%). In contrast, no triploid embryos were detected in HA89 (0%; 95% CI: 0–12.3%; $n = 35$; Fig. 1, J). The formation of triploid progeny could be one of the causes of the high abortion rate detected in Rf975. Since Rf975 produces normal pollen of uniform size (see below) and non-reduced (AES-like) female gametophytes¹⁶, we concluded that the triploid progeny was likely BIII (2n + n) hybrids, formed following the fertilization of the AES by a normally reduced (n) male gamete.

Rf975 forms viable BIII (2n + n) progeny

The progeny derived from the self-pollination of Rf975 (aposporous) and HA89 (sexual) lines was grown under controlled conditions, and leaves at the V2 developmental stage were collected²⁸. Ploidy level analysis of 51 Rf975-derived plantlets identified eight triploid individuals (15.68%; 95% CI: 7.49–29.14%). No triploids were detected among 65 HA89 progeny plants (0%; 95% CI: 0–6.95%). Next, immature embryo rescue was performed to try to avoid developmental collapse due to endosperm imbalance in the BIII hybrids. Of 240 rescued Rf975

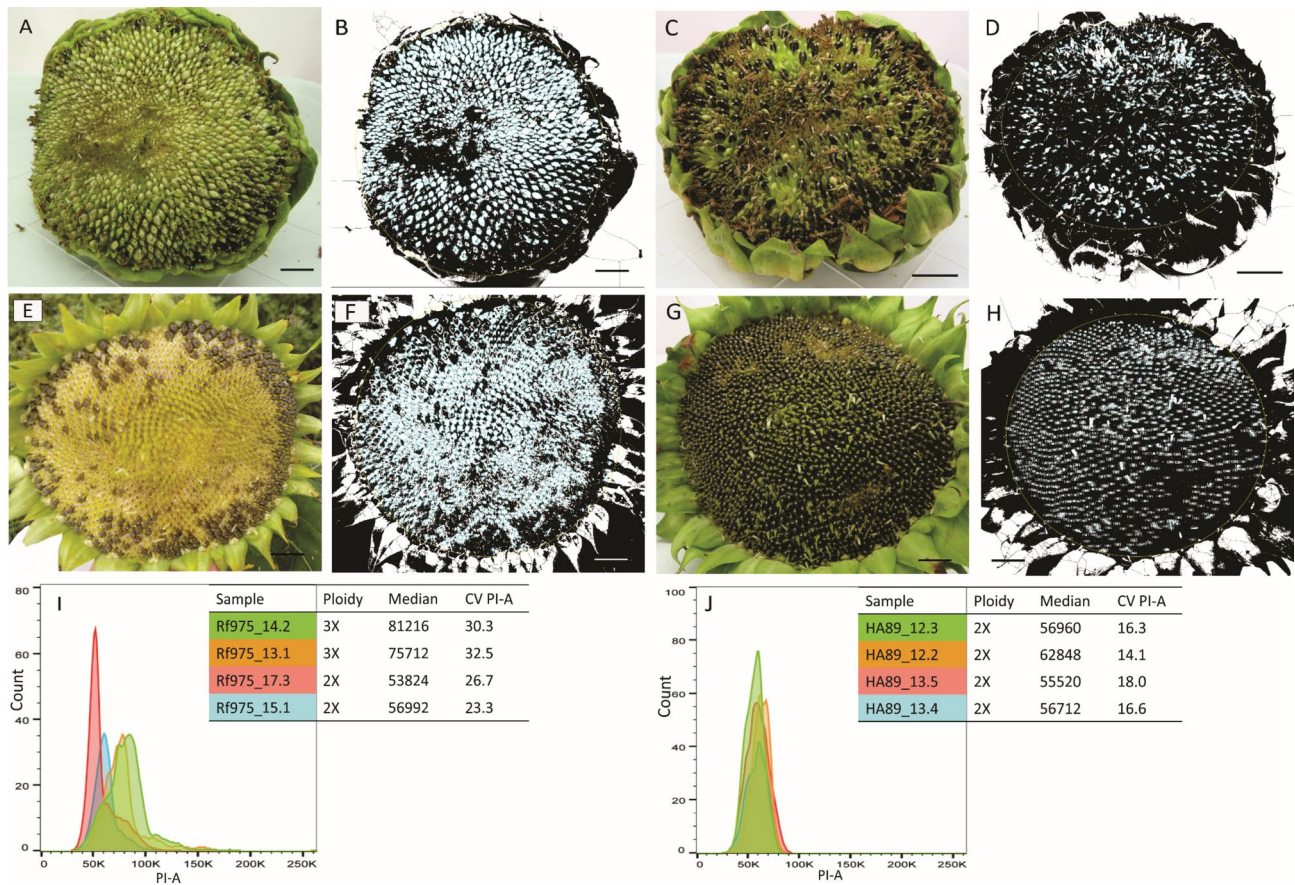


Fig. 1. Seed counting in Rf975 and HA89 capitula at different developmental stages (R6 and R8) and flow cytometry analysis of R6 developing embryos. (A–D) Photographs of capitula (A,C) and image analysis outputs (B,D) from the Rf975 line at R6 (A,B) and R8 (C,D) developmental stages. The corolla, anthers, and style/stigma were removed. (E–H): Photographs of capitula (E,G) and image analysis outputs (F,H) from the HA89 line at R6 (E,F) and R8 (G,H) developmental stages. (I,J): Flow cytometry analysis of ovaries from Rf975 (I) and HA89 (J) at R6. Ploidy level, median PI-A (propidium iodide fluorescence) value, and coefficient of variation (CV) are shown alongside the graphs. Scale bars = 2 cm.

embryos, 54 progressed to the reproductive stage. From this group, eight plants were classified as triploids (14.8%; 95% CI: 6.1–27.6%, $n=54$) and 46 as diploids. In contrast, of the 120 cultivated embryos from the diploid HA89 sexual line, only 26 reached the vegetative phase, and all were diploid (100%; 95% CI: 84–100%, $n=26$). The experiment was replicated over two independent growing seasons (2021–2022 and 2022–2023), yielding similar embryo rescue efficiencies. These results indicate that only a small proportion of the Rf975 triploid embryos reach maturity. Embryo rescue techniques do not increase this number, at least when immature achenes are dissected 10 days after anthesis (E4 phenophase).

Phenotypic characterization of triploid and diploid Rf975

Plants derived from self-pollinated mature seeds of Rf975 and HA89 lines were grown under controlled conditions. The Rf975 progeny included diploid and triploid individuals, whereas the HA89 progeny consisted only of diploids. Phenotypic analysis of vegetative traits (plant height, leaf area) revealed no significant differences either between triploids and diploids or between Rf975 and HA89 diploids (Table 1). However, a significant reduction in seed production was observed in triploid Rf975 plants compared to diploid ones (Table 1). The number of days to reach the R1 stage was also slightly, but significantly, reduced in triploids compared to diploids (Table 1). Cytoembryological analysis was performed on disc flowers from diploid and triploid Rf975 genotypes, spanning flower bud stage (E1) to post-anthesis (E4) phenophases. All triploid plants studied exhibited at least one ovule containing one or more aposporous embryo sacs (AES); therefore, they were classified as aposporous individuals (100%; 95% CI: 46.3–100%, $n=5$; Table 1). AESs were predominantly detected at later developmental stages (E3–E4 phenophases) (Fig. 2A, C). Sometimes, they were located in the position usually occupied by the antipodal cells, but they morphologically differ from them due to their round shape and the presence of fused polar nuclei. In contrast, in diploid Rf975 plants, most ovules displayed meiotic embryo sacs (Fig. 2D), similar to those observed in HA89 2x control plants (Fig. 2F). Only 10% (95% CI: 0.5–45.8%, $n=10$) of diploid Rf975 plants exhibited at least one ovule containing one or more AESs (Table 1). The average number of ovules exhibiting AES in triploid plants was 61.9% (95% CI: 38.7–81.04%, $n=21$), compared to 4.55 (95% CI: 0.2–24.9%, $n=22$)

Genotype	Ploidy level	PI-A median	Plant height (cm)	Leaf area (cm ²)	Days to R1	Capitulum diameter (cm)	Seed number/capitulum	Apospory Penetrance	Apospory Expressivity
Rf975	2x	40,750 ± 1890	33.85 ± 1.14	8.05 ± 0.58	40.28 ± 0.28	3.61 ± 0.15	49.8 ± 8.6	10% (0.5–45.8%)	4.55% (0.2–24.9%)
Rf975	3x	61,771 ± 1927	33.63 ± 1.47	7.87 ± 0.32	41.87 ± 0.85	3.88 ± 0.29	20.4 ± 6.3	100% (46.3–100%)	61.9% (38.7–81%)
t-test Rf975-2x vs. Rf975-3x		2e-6*	0.90	0.36	0.04*	0.30	0.01*		
HA89	2x	37,400 ± 2288	35.31 ± 0.85	7.11 ± 0.44	40.12 ± 0.29	3.19 ± 0.290	35.2 ± 12.4	0% (0–21.8%)	0% (0–12.6%, n = 34)
t-test Rf975-2x vs. HA89		0.32	0.38	0.08	0.71	0.16	0.38		

Table 1. Vegetative and reproductive phenotypic traits studied in self-pollinated parental lines cultivated under greenhouse conditions. *Asterisk indicate significant differences ($\alpha < 0.05$). Plant height (cm), leaf area (cm²), days to R1, capitulum diameter (cm), and seed number/capitulum were evaluated in a non-balanced assay involving the following number of plants (n): Rf975-2x n = 30; Rf975-3x n = 8; HA89-2x n = 30. Apospory penetrance was evaluated in a non-balanced assay involving the following number of plants (n): Rf975-2x n = 10; Rf975-3x n = 5; HA89-2x n = 10. Apospory expressivity was evaluated in a non-balanced assay involving the following number of ovaries (n): Rf975 2x n = 22; Rf975-3x n = 21; HA89-2x n = 34.

in diploid plants (Table 1). These findings suggest that apospory is enhanced in triploids compared to diploid Rf975 plants. Additionally, pollen abnormalities, including size and shape variations, were observed in most triploid plants (Fig. 2B), while pollen in diploids was uniform (Fig. 2, E) and similar to that observed in HA89 2x control plants (Fig. 2G). One triploid individual did not survive to the flowering stage (R5.5 developmental stage, according to Schneiter and Miller²⁸), and insufficient ovary collection prevented a definitive classification for two other plants. It is important to note that a critical issue with this material is that triploids produce few mature seeds, and many must be preserved for future cultivation, significantly reducing the number of ovules available for analysis.

Next, immature embryo rescue plants, classified as diploid or triploid by flow cytometry (Fig. 2H), were cytoembryologically analyzed. As in the previous analysis, phenotypic evaluation of vegetative traits (plant height, leaf area) revealed no significant differences either between Rf975 triploids and diploids, or between Rf975 and HA89 diploids (Table 2). Regarding reproductive phenotypes, triploid Rf975 plants exhibited a high frequency of ovules containing aposporous embryo sacs (AES) (100%; 95% CI: 51.7–100%, n = 6) (Fig. 2I). In contrast, the HA89 genotype exhibited typical sexual embryo sacs (Fig. 2J). The triploid plants also displayed abnormal or scarce pollen grains and produced few or no seeds (Fig. 2K). In contrast, the HA89 genotype exhibited normal pollen (Table 2). A comparison between triploids derived from mature seed sowing and those obtained via embryo rescue revealed that, while plant height was similar, the latter had significantly smaller capitulum diameters, lower seed production, and increased susceptibility to pathogens. These observations underscore the negative impact of the embryo rescue technique on plant fertility and suggest that it is unlikely to be effective for producing a larger number of triploids in these lines.

Apomictic development assessment using SNP-based progeny test

We established a progeny test assay to investigate the potential of the diploid line Rf975 for completing the entire apomixis process (apospory + parthenogenesis). A crossing scheme was implemented using the facultative aposporous diploid Rf975 line as the female parent and the sexual diploid HA89 line as the pollen donor. The parental lines are genetically divergent homozygous lines. The generation of a diploid hybrid F₁ progeny, derived from the fertilization of reduced Rf975 female gametophytes with reduced HA89 pollen, was necessary to facilitate subsequent segregation analysis in the F₂ generation. The F₁ progeny displays heterozygous loci, representing the polymorphic alleles derived from Rf975 and HA89 inbred lines. If seeds are produced sexually, during the self-pollination of the F₁ progeny, necessary to produce the F₂ progeny, different genetic constitutions may arise, depending on the reproductive mode used to produce the seeds. The reduced female and male gametes (both originating from the heterozygous F₁) will combine, generating a new individual with a unique genetic constitution, in which some of the F₁ alleles may be lost due to random segregation. Conversely, if seeds are produced through apomixis, the F₁ pollen may be used to generate the endosperm via pseudogamy, but the embryo will form directly from a non-reduced F₁ female gamete and will therefore carry the original F₁ genetic constitution. Thus, identifying F₂ plants with the F₁ (maternal) genotype would indicate apomictic reproduction.

First, the cytoembryology of diploid Rf975 × HA89 F₁ hybrids was examined. Analysis of 11 plants revealed the presence of aposporous embryo sacs in seven of them, indicating a penetrance of the trait of 63.6% (95% CI: 31.6–87.6%, n = 11). Therefore, these seven plants were classified as aposporous. No AESs were detected in the remaining four plants, so they were classified as sexual. The expressivity of apospory in the seven apomictic F₁ hybrids was 7.8% on average (95% CI: 3.9–14.8%, n = 114), i.e., out of a total of 114 ovules analyzed, nine displayed aposporous embryo sacs. These numbers are consistent with the data reported by Menéndez et al.¹⁶. The cytoembryological analysis of diploid Rf975 × HA89 F₁ hybrids is shown in Fig. 3A–D. Both meiotic sacs (Fig. 3A) and well-developed aposporous embryo sacs coexisting with the meiotic sacs (Fig. 3B–D) were observed.

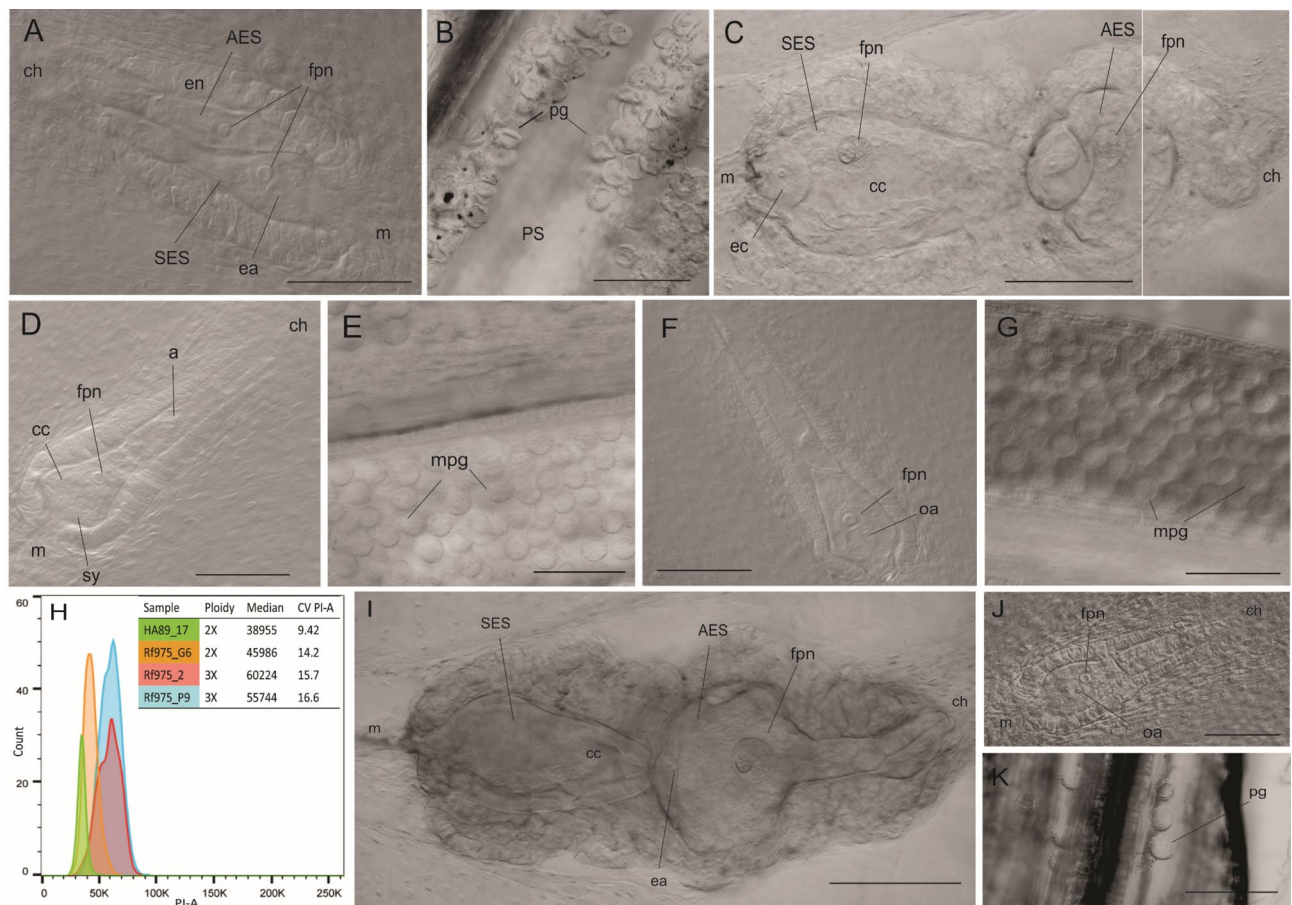


Fig. 2. Cytoembryological analysis of diploid and triploid Rf975 plants. (A–G) Plants obtained by ground-sowing. (H–K) Plants obtained by immature embryo rescue. (A–C) Reproductive organs of triploid Rf975 plants. (D,E) Reproductive organs of diploid Rf975 plants. (F,G) Reproductive organs of diploid sexual HA89 plants. (A) Sexual embryo sac (SES) and aposporous embryo sac (AES), surrounded by the endothelium (en), with visible egg apparatus (ea) and fused polar nuclei (fpn) in both embryo sacs. The micropylar (m) and chalazal (ch) poles are indicated. The SES developed from the chalazal megasporangium, while the megasporangia at the micropylar end have degenerated. (B) Sparse and variable-sized pollen grains (pg) in the pollen sac (PS) of triploid plants. (C): Left: ovule containing a sexual and an aposporous embryo sac (SES and AES, respectively), ec: egg cell. Right: distal portion of the same AES shown in the previous image. (D) Single sexual embryo sac with synergid cells (sy), central cell (cc), fused polar nuclei (fpn), and antipodal cells (a). The micropylar (m) and chalazal (ch) poles are indicated. (E) Mature pollen grains (mpg) of uniform size. (F) Typical *Polygonum*-type embryo sac (from HA89 2x control plants). (G) Uniform mature pollen grains (from HA89 2x control plants). (H) Flow cytometry analysis of V2 leaves from Rf975 3x, Rf975 2x, and HA89 2x plants. The median of the PI-A (propidium iodide fluorescence) and the Coefficient of Variation (CV) are included. (I) Ovule of Rf975 3x: an aborted sexual embryo sac (SES) with central cell (cc) near the micropylar (m) region and an aposporous embryo sac with the egg apparatus (ea) and fused polar nuclei (fpn), near the chalazal region (ch). (J) Rf975 2x meiotic sexual embryo sac, with egg apparatus (ea) and fused polar nuclei (fpn). The three degenerating megasporangia appear to be crushed against the micropyle. (K) Sparse pollen grains (pg) in the pollen sac of Rf975 3x. Bars: 100 μ m.

Seeds from self-pollinated F_1 plants were collected and planted to generate a segregating F_2 population carrying alleles from both Rf975 and HA89. Within the F_2 generation, most plants were diploid (2x) (F_2 -2x), but triploid (3x) plants (F_2 -3x) were identified at a frequency of 13.4% (95% CI: 4.54–32.1%; $n = 23$). Additionally, some F_1 plants (designated F_1 -E) were emasculated and bagged to explore the potential occurrence of autonomous apomixis in the F_1 hybrids. A few seeds (designated F_2 -E) were collected from these emasculated F_1 plants, with two possible origins: autonomous apomixis or pollen escape. These seeds were cultivated to generate F_2 -E mature plants, which were subsequently included in the (epi)genetic profiling analysis.

Genetic and DNA methylation profiles were performed using the MCSEED-based method²⁹ on parental lines Rf975 and HA89, 3 diploid F_1 hybrids, and 17 diploid F_2 progeny (F_2 -2x and F_2 -E). To identify SNPs present or absent across different samples, we retained all variants detected in the crosses without applying additional filtering, except for a minimum coverage threshold of > 10 per locus. This approach enabled us to capture SNPs that were present in some samples but absent in others. Following this base-calling analysis, we identified 59,792

Genotype	Ploidy level	PI-A median	Plant height (cm)	Days to R1	Capitulum diameter (cm)	Seed number/capitulum	Apospory penetrance	Apospory expressivity
Rf975	2x	40,872 ± 1190	32.5 ± 1.75	36.12 ± 0.39	1.96 ± 0.33	6.4 ± 1.3	0% (0-43.9%)	0% (0-30.1%)
Rf975	3x	61,062 ± 1570	33.33 ± 3.5	36.33 ± 0.6	1.84 ± 0.17	2.22 ± 1.39	100% (51.7-100%)	69.2% (38.9-89.6%)
t-test RF975-2x vs. RF975-3x		1e-09*	0.377	0.26	0.377	0.053		
HA89	2x	38,655 ± 1076	36.16 ± 2	36 ± 0.36	1.77 ± 0.11	14 ± 4.79	0% (0-53.7%)	0% (0-25.4%)
t-test RF975-2x vs. HA89		0.083	0.126	0.139	0.43	0.068		

Table 2. Phenotypic traits studied in Rf975 and HA89 plants obtained by immature embryo rescue. *Asterisk indicate significant differences ($\alpha < 0.05$). Plant height (cm), leaf area (cm^2), days to R1, capitulum diameter (cm), and seed number/capitulum were evaluated in a non-balanced assay involving the following number of plants (n): Rf975-2x n = 7; Rf975-3x n = 6; HA89-2x n = 9. Apospory penetrance was evaluated in a non-balanced assay involving: Rf975-2x n = 7; Rf975-3x n = 6; HA89-2x n = 5. Apospory expressivity was evaluated in a non-balanced assay involving the following number of ovaries (n): Rf975-2x n = 12; Rf975-3x n = 13; HA89-2x n = 15.

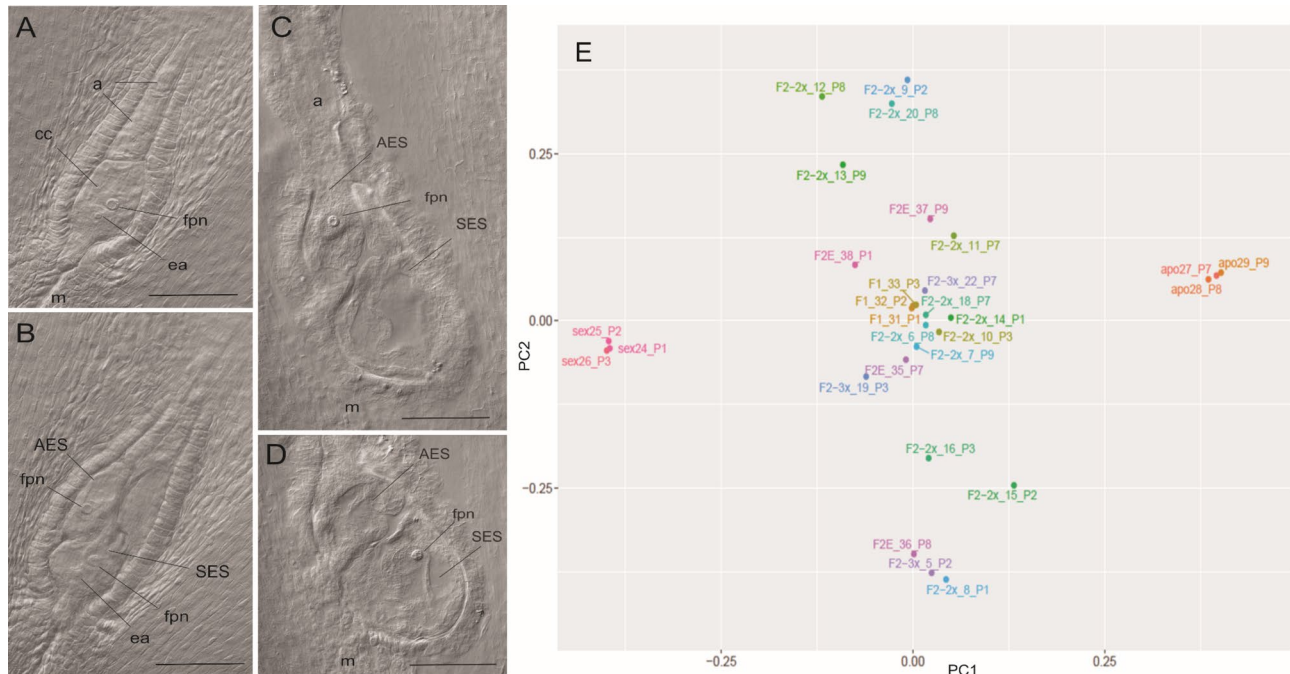


Fig. 3. Progeny test principal component analysis and cytoembryological analysis of Rf975 × HA89 hybrids. (A) Canonical single sexual embryo sac. The central cell (cc), fused polar nuclei (fpn), and egg apparatus (ea) are visualized at the micropylar region (m); antipodal (a) are visible at the distal end. The three degenerating megasporic remnants appear to be crushed against the micropyle. (B–D) Aposporous embryo sac (AES) with fused polar nuclei (fpn), adjacent to the canonical sexual embryo sac (SES) with antipodal cells (a), fused polar nuclei (fpn), and egg apparatus (ea). Bars: 100 μm . (E) Principal component analysis of molecular markers obtained from the MCSeED-based experiment, representing the genetic/epigenetic distances among the progenitors (Rf975: experimental codes apo27-28-29; HA89: experimental codes sex 24-25-26) and F₁, F₂-2x, and F₂-3x plants.

SNPs (Supplementary Table S1). Principal component analysis (PCA) revealed that the first and second principal components explained 7.2% and 2.3% of the total variation, respectively (Fig. 3E). As expected, this analysis confirmed the presence of alleles from both Rf975 and HA89 in the F₁ population. The genetic profiles of the F₁ hybrids were highly similar but not identical, suggesting that non-conserved genetic changes occurred after hybridization, as described in the literature for other species^{30–32}. No F₂ individuals exhibited genetic patterns identical to the F₁ genotypes, suggesting that apomixis cannot be completed at the diploid level (Fig. 3E). One plant from the F₂-2x group (namely F₂-18-P7) exhibited a genetic pattern similar to the F₁ and was therefore marked as a potential clonal progeny. However, analysis of a highly informative SNP subgroup (comprising 5,177

Loci location	Ploidy- specificity	<i>H. annuus</i> sequence ID	eV	Query cover (%)	<i>H. annuus</i> L. annotation
Chr1-7076494	3x	KAF5762472.1	0.0	100	putative retrotransposon gag domain, aspartic peptidase domain superfamily
Chr4-57374684	3x	KAJ0567750.1	6e ⁻⁴⁷	15	putative retrotransposon gag domain-containing protein
Chr4-71286193	3x	KAF5779213.1	0.0	99	putative nucleotidyltransferase, RibonucleaseH
Chr9-183592207	3x	KAJ0948431.1	7e ⁻³⁷	12	hypothetical protein HanRHA438_Chro01g0027151
Chr11-9462048	2x	XP_021990966.1	0.0	84	protein FAR1-RELATED SEQUENCE 5-like
Chr16-187730844	3x	KAJ0642001.1	0.0	87	putative Heat shock protein 70 family

Table 3. Ploidy-specific *H. annuus* loci identified by MCSeED-based experiment.

SNPs, which were dominant homozygous in one parent, recessive homozygous in the other parent, heterozygous in the F_1 , and segregating in the F_2) identified 943 molecular markers that differed between F_2 -18-P7 and the F_1 genetic pattern. Consequently, the apomictic origin of F_2 -18-P7 was ruled out (Supplementary Table S2). Furthermore, the F_2 -E profiles exhibited segregation patterns that originated from both parental plants, leading to the conclusion that these plants did not originate from autonomous apomixis, but from pollen escape. Altogether, our results suggest that, although the diploid Rf975 and the derived diploid F_1 hybrids are capable of non-reduced embryo sac formation (apospory), they do not complete parthenogenesis and, therefore, cannot be classified as apomicts.

Identification of recurrent (epi)genetic mutations during polyploidization

Additionally, we used the MCSeED data to compare the genetic and DNA methylation profiles of the parental diploid (2x) lines Rf975 and HA89 (each with three biological replicates), three diploid F_1 plants (2x), 17 diploid F_2 plants (F_2 -2x and F_2 -E), and three triploid F_2 plants (F_2 -3x). This comparison aimed to identify genetic and/or epigenetic variations that recurrently occurred in several independent polyploidization events (such as insertions, deletions, or cytosine methylations). Specifically, we focused on genetic and DNA methylation polymorphisms in the CHG context that were present or absent exclusively in triploids. In total, 23 diploid and 3 triploid individuals were compared. Our analysis identified six genomic loci exhibiting a ploidy-specific pattern, represented by sequence reads that were present or absent solely in triploids (Supplementary Table 3). These variations may have arisen from sequence polymorphisms or differential cytosine methylation at a PstI (CHG context) site. The identified (epi)mutated genomic regions were compared with annotated *Helianthus annuus* L. sequences (Table 3). The polymorphic sequences were primarily associated with mobile elements and were annotated as retrotransposon gag domain, aspartic peptidase domain superfamily, nucleotidyltransferase ribonuclease H, heat shock protein 70 family, and FAR1-related sequence 5-like (Table 3).

We also investigated SNP loci that occurred only in triploid or only in diploid plants. A total of 5,177 SNP markers exhibiting alternative homozygosity (0/0 and 1/1) in the parents, heterozygosity (0/1) in the F_1 progeny, and segregation in the F_2 generation were selected for this study. Given their origin from unreduced maternal gametes, these markers were expected to be heterozygous in triploids (1/1/0 or 0/0/1). However, out of the 5,177 total markers, we identified 241 that unexpectedly displayed a homozygous pattern (0/0/0 or 1/1/1) in all triploid replicates. These 241 markers are candidates for having undergone recurrent genetic changes following the ploidy increase, resulting in the mutation of one allele. Interestingly, although SNP markers are expected to be randomly distributed, these recurrent mutations were predominantly clustered on chromosome 12 (89 loci affected), with a few occurring on chromosomes 1 (1 locus) and 16 (2 loci). The number of point mutations per locus ranged from 1 to 12, indicating that some genes contained up to 12 point-mutations recurrently found in triploid genotypes. A significant portion of these mutations (23% of the mutations on chromosome 12 and 50% of those on chromosome 16) occurred within introns of putative leucine-rich repeat/malectin receptor-like kinase genes (similar to GenBank accession MN990444.1). Of the 241 total polymorphisms, 143 were found to occur in sequences that display some degree of similarity with sequences previously reported to be associated with physiological traits, such as response to biotic and abiotic stress, hormone regulation and transport, development, cell death induction, ribosome biogenesis, DNA replication, and chromatin remodeling (Supplementary Table S3). Overall, our results suggest that during sunflower triploidization, recurrent non-random mutations affect specific loci located mainly on chromosome 12, some of which may have physiological impact and could be associated with the unique phenotype observed in triploids.

Discussion

In higher plants, sexual reproduction and apomixis have evolved together as alternative reproductive strategies, and are currently considered possible ancestral polyphenic traits that are often modulated by polyploidy³³. The transition from sexual to apomictic reproduction is regulated by a variety of mechanisms that control gene expression, translation, and protein function, potentially triggered by an increase in the number of chromosomal sets³³. Recent studies have highlighted a surprising degree of conservation in the molecular pathways regulating sexual and asexual reproduction across flowering plant families³⁴. Epigenetic regulation, cell cycle control, hormonal signalling, and signal transduction processes appear to be interconnected as key elements in this reproductive transition^{34–36}.

The research presented here confirms the existence of natural apospory (i.e., the first step of aposporous apomixis development) in cultivated sunflower, as suggested by Voronova¹⁷ and Menendez et al.¹⁶. Previous studies by these authors identified structures resembling AES in specific wild and cultivated genotypes.

However, those studies failed to confirm the unreduced nature of these abnormal megagametophytes^{16,17}. The present study investigated the viability and ploidy of these AES-like structures, as well as the interactions among polyploidization, subsequent genomic alterations, and the establishment of reproductive modes (apospory and parthenogenesis) in the cultivated sunflower line Rf975. Our first finding was the detection of numerous triploid BIII hybrids in the progeny of the diploid line Rf975, whose cytoembryology had previously revealed aposporous-like embryo sacs¹⁶. This confirmed the occurrence of non-reduced female gametophytes in Rf975 and demonstrated that these non-reduced gametophytes are fully viable and capable of forming embryos after fertilization. The possibility of triploids arising from fertilization events involving unreduced microgametophytes is highly unlikely, as the pollen produced by Rf975 is uniform in size and shape, closely resembling that of the control line HA89.

Triploids derived from Rf975 exhibit specific phenotypic traits, including delayed blooming, abnormal pollen formation, and poor seed set. Moreover, our cytoembryological analyses revealed an increased proportion of ovules containing aposporous embryo sacs (100% of the analysed triploid plants) compared to diploid aposporous plants of the same line Rf975 (approximately 10%). The well-established association between apomixis and polyploidy³⁷ is characterized by an increase in both the frequency and intensity of apomixis with rising ploidy levels¹⁸. As an archetypal example, in natural populations of subtropical apomictic *Paspalum* spp., diploids are generally sexual but may occasionally exhibit very low levels of apospory in the absence of parthenogenesis. Triploids are partially sterile facultative apomicts, and tetraploids are facultative or obligate apomicts^{35,38}. In angiosperms, seeds originating from diploid plants generally contain diploid embryos and triploid endosperm as a result of double fertilization^{39,40}, requiring a 2 m:1p maternal: paternal genomic balance in the endosperm for successful development^{39,41}. Fertilization of non-reduced female gametophytes by reduced pollen nuclei results in 3x embryos and 5x (4 m:1p) endosperm, leading to developmental collapse. This could be the most likely explanation for the high number (42.8%) of triploid embryos detected in the Rf975 progeny at early developmental stages, with only a small proportion (36.6%) germinating and reaching maturity. While conducting this study, we hypothesized that immature embryo rescue could enhance the successful recovery of triploid plants derived from Rf975, by potentially bypassing endosperm-related developmental issues. However, the proportion of triploids recovered through the embryo rescue assay was similar to that obtained from mature seed culture, and their phenotypic traits were inferior (reduced capitulum size, lower seed set). This technique could be tested at earlier developmental stages, for example, rescuing embryos at the E4 phenophase instead of the E5 phenophase¹⁶, to increase the likelihood of success.

We further explored the occurrence of complete apomixis (apospory + parthenogenesis) in the Rf975 line. In apomictic species, at high ploidy levels, the maternal: paternal contribution to the endosperm is not strictly controlled, facilitating the formation of clonal maternal seeds. In fact, the embryo/endosperm ploidy ratio is often used to determine the origin of seeds (sexual vs. apomictic), but this method is not applicable to species where the endosperm is consumed immediately after fertilization, such as sunflower (revised in Doll and Ingram⁴²). Attempts to estimate the embryo/endosperm ploidy ratio in immature R8 sunflower seeds from diploid Rf975 using flow cytometry were unsuccessful, as the endosperm peak could not be easily detected at this developmental stage. As a result, a genetic and epigenetic approach was employed to analyse the progeny and identify potential apomictic offspring exhibiting the maternal genotype. Cytoembryological analysis confirmed that the aposporous capacity of the maternal line was retained in the F₁ hybrid progeny. Three diploid F₁ individuals were selected and allowed to self-pollinate to form a diploid segregant F₂ population. We analyzed the SNP genetic profiles of 21 F₂ plants to identify individuals with the hybrid F₁ constitution (i.e., maternal offspring), but all F₂ plants segregated the alleles present in the F₁ (i.e., they lacked some of the Rf975 and HA89 alleles present in the F₁). Of the 17 F₂ plants analyzed, none was classified as originating from maternal reproduction (0%, 95% CI: 0–0.1843). According to the 95% confidence interval of the proportion, we cannot exclude levels of apomixis below 18% with this analysis. Based on this test and the previous cytoembryological evidence, we concluded that Rf975 is aposporous but not parthenogenetic and, therefore, cannot complete apomixis. However, the number of F₂ individuals tested was not large enough to rule out the possibility of low levels of apomixis (below 18%) in diploid Rf975. Further exploration of complete apomixis (apospory + parthenogenesis) at the triploid level would have required sexual crosses with genetically divergent genotypes. This was an unattainable objective, as triploids frequently form aneuploid gametes, complicating progeny generation and result analysis. Future studies involving the induction of tetraploidy in Rf975 through colchicine treatment will facilitate the investigation of apomixis by using progeny tests at higher ploidy levels.

The MCSeEd method applied to the progeny test enabled additional genetic and DNA methylation analyses aimed at detecting (epi)genetic variations occurring during triploidization. These changes included the loss or gain of specific sequences, methylation or demethylation, and recurrent point mutations, which do not appear to occur randomly. Epigenetic changes consistently involved transposable elements and involved loci located in different chromosomes. On the contrary, genetic mutations (specifically, point nucleotide mutations) were concentrated in a specific region of sunflower chromosome 12, suggesting the presence of a potential hotspot for recurrent genetic rearrangements during triploidization events. Interestingly, some mutations were found in genes linked to stress response and disease resistance, which could influence the adaptation of triploid plants. This list of genes that are recurrently mutated during sunflower triploidization may provide promising candidates for traits related to polyploidy, including abiotic and biotic stress tolerance and changes in reproductive behaviour. Previous examples of recurrent mutations occurring after polyploidization have been reported in *Eragrostis curvula*⁴³ and *Paspalum plicatum*⁴⁴, but the genomic location and nature of the involved loci were not investigated.

This study reveals the formation of triploid BIII hybrids in the sunflower line Rf975, derived from the fertilization of unreduced female gametes. It proves that both the expressivity and penetrance of apospory are increased in Rf975 triploids compared to Rf975 diploids, and identifies genetic/epigenetic sequences that

are recurrently mutated in response to the change in ploidy from 2x to 3x. Challenges remain regarding the presence of apomixis (i.e., formation of viable clonal progeny) at the triploid level, but according to the MCSeED progeny tests, diploid Rf975 do not produce maternal seeds at levels > 18%. These results will contribute to the ongoing characterization of the trait at higher ploidy levels (e.g., in tetraploids) and to future research aimed at utilizing apomixis for sunflower breeding. Moreover, exploring the genes and regulatory pathways associated with apomixis expression in Rf975 plants at different ploidy levels will provide valuable insights for developing sunflower breeding strategies.

Methods

Plant material

The starting plant material consisted of the following lines: (1) a public inbred line HA89 released by USDA-ARS, USA (2x, sexual control); and (2) an inbred line developed by the Estación Experimental Agropecuaria (EEA) Instituto Nacional de Tecnología Agropecuaria (INTA) Pergamino, Argentina, Rf975 (2x, aposporous-like)¹⁶. Plants were seeded in the field, under irrigation and manual weed control, and in the greenhouse under controlled light and temperature conditions, in the experimental facilities of Facultad de Ciencias Agrarias, Universidad Nacional de Rosario, Argentina. Rf975 × HA89 crosses were made by manual emasculation of Rf975 capitula at R5.1 stage²⁸ using HA89 as pollen donor. Thirty plants of the F₁ progeny were cultivated: fifteen of them were emasculated and bagged, while the remaining 15 were bagged to allow self-pollination. Reproductive tissue samples for embryological studies and mature seeds were collected at stages R5.5 and R8²⁸.

Bioinformatic quantification of young fruits and developing seeds

Capitulum developmental stages were assessed according to Schneiter and Miller²⁸. The number of young fruits (ovaries at the R6 stage) and developing seeds (at the R8 stage) was estimated in 25 capitula per line (Rf975 and HA89) using image analysis²⁷. The assays were repeated over three seasons (2021/2022, 2022/2023, and 2023/2024), and means were compared using Student's t-test, after verifying normal distribution and homogeneity of data variance (Shapiro-Wilk and Levene's tests), with data analysis performed using R software⁴⁵.

Flow cytometry analyses

A total of 35 embryo samples per genotype were analysed, each containing 2–3 embryos dissected from R6 ovaries under a stereomicroscope (Optyka SZM-LED2, Optyca Microscopes). Additionally, leaf tissue samples were collected from 30 plants of each parental line and hybrid at the V4 stage²⁸. Nuclei suspensions were prepared according to the Otto protocol⁴⁶, and stained with a 1 mg/mL propidium iodide (PI) solution, following neutralization with Otto buffer 2 (0.4 M Na₂HPO₄). Flow cytometry was used to determine the ploidy level of individual plants, as described by Kallamadi and Mulpuri⁴⁷. Analyses were performed on a BD FACSaria II flow cytometer (BD Biosciences) at Instituto de Fisiología Experimental, CCT-ROSARIO, Argentina. The relative DNA content of each sample was estimated by comparing fluorescence intensity profiles to those of the HA89 2x control, using the FlowJo v10.8.1 software⁴⁸ (BD Biosciences).

Phenotypic characterization of lines and hybrids

Vegetative variables included plant height and the leaf area of the first pair of leaves at the V4 developmental stage. Reproductive variables included the number of days to reach the R1 stage, the capitulum size at the R5 stage, and the number of seeds produced. Reproductive phenotypes were characterized through cytoembryological analysis using Differential Interference Contrast (DIC) microscopy, as described by Menéndez et al.¹⁶. Disc flower samples were collected during phenophases E1 to E5 at the R5 stage (according to Menéndez et al.¹⁶), fixed in modified FAA⁴⁹ for 24 h, and clarified using Herr's Jr⁵⁰. protocol. Observations were made using a DIC-Leica DM 2500 microscope (Leica Microsystems).

Immature embryo culture assay

The non-sterile germination method described by Breccia et al.⁵¹ was used to obtain plantlets from immature embryos. Achenes were dissected from ovaries 10 days after anthesis (daa) of Rf975 and HA89 genotypes. Embryos were cultured in small plastic trays filled with sterile sand, irrigated by capillarity with MS nutrient solution⁵², and maintained in a growth chamber at 25 ± 2 °C, 70% relative humidity, and a 16/8 light/dark cycle for 15 days. Plantlets were then transferred to 20 L pots and grown in a greenhouse with controlled light, temperature, and humidity until flowering. The assay was repeated over two growing seasons (2021/2022 and 2022/2023).

Genetic profiling

Rf975 is a stabilized inbred line, apomixis-derived progeny would not differ genetically from progeny obtained via self-pollination. Therefore, it was crossed with the genetically divergent sexual line HA89 to generate F₁ hybrids. After crossing Rf975 × HA89, the genetic profiles of the parental lines, the derived F₁ hybrids, and the F₂ progeny were analysed using a Methylation Context Sensitive Enzyme ddRAD (MCSeED)-based approach²⁹. Leaf samples were collected at the V4 stage, weighed, and stored at – 80 °C. Genomic DNA was extracted from three biological replicates per genotype using the Wizard® Genomic DNA Purification Kit (Promega). DNA integrity was assessed by running 1% (w/v) agarose gels. MCSeED libraries were prepared following the methodology described by Marconi et al.²⁹. The PstI + MseI endonuclease combination was used for restriction digestion. The restriction and adapter ligation steps were performed for all samples as outlined by Marconi et al.²⁹, grouping them according to five different Illumina adapter indexes (Index 2, 4, 5, 6, and 7). DNA fragments were precipitated, bound to magnetic beads (AMPure XP, Beckman Coulter), and resolved on a 1% agarose gel. DNA fragments ranging from 250 to 700 bp were excised from the gel and purified using the QIAquick

Gel Extraction Kit (Qiagen). The grouped libraries were pooled in equimolar proportions, and the final library was sequenced on an Illumina platform using 150-bp paired-end chemistry. Sequencing was performed in one lane on an Illumina Novaseq 6000 platform from both directions (2×150 bp) at Novogene (Cambridge, UK). The sequence data was deposited in the NCBI Sequence Read Archive under BioProject ID: PRJNA1162057. Raw reads from the Illumina sequencing were demultiplexed using the process_radtags tool (STACKS v.2.3b package⁵³, and variant calling was conducted according to the MCSEED pipeline²⁹. The resulting VCF file, containing frequencies and reference/alternative alleles, was used to identify polymorphic markers between the parental lines, which would allow the identification of heterozygotes in the F_1 hybrids and segregants (indicative of sexual reproduction) or non-segregants (indicative of apomixis) in the F_2 progeny. The identity-by-state distance matrix was calculated using PLINK v1.07 software⁵⁴. This matrix was used to generate a Principal Component Analysis (PCA) plot and a dendrogram using R version 3.3.2 (www.r-project.org) with the 'factoextra' and 'pvclust' packages, respectively. SNPs that were homozygous in the parents, heterozygous in all F_1 individuals, segregant in F_2 diploids and homozygous in all F_2 triploids were analyzed to identify non-random genetic changes associated with triploidization. Since F_2 triploids result from the fertilization of non-reduced female embryo sacs produced by heterozygous F_1 individuals, they are expected to be heterozygous. Therefore, the observed homozygosity in all triploids suggests recurrent genetic mutations at the alternative allele. The 2 kb regions flanking the detected polymorphisms (± 1 kb) were recovered from the Sunflower Genome Database (<https://sunflowergenome.org/> using JBrowse, HA412-HOv2.0 Assembly), and BLASTX and BLASTN analyses were performed against the non-redundant sequence database for *Helianthus annuus* (taxid: 4232) at NCBI (<https://blast.ncbi.nlm.nih.gov/Blast.cgi>).

Data availability

The sequence data was deposited in the NCBI Sequence Read Archive under BioProject ID: PRJNA1162057. The plant material used in this study are available under request to EEA-Pergamino (INTA), Argentina (www.argentina.gob.ar/inta/cr-buenosaires-norte/eea-pergamino) and USDA-ARS, USA (www.ars.usda.gov). The datasets generated during and/or analysed during the current study are available from the corresponding author on reasonable request.

Received: 8 November 2024; Accepted: 3 February 2025

Published online: 09 February 2025

References

1. Adeleke, B. S. & Babalola, O. O. Oilseed crop sunflower (*Helianthus annuus*) as a source of food: Nutritional and health benefits. *Food Sci. Nutr.* **8** (9), 4666–4684 (2020).
2. Filho, D. O., Egea, M. B. & J.G. & Sunflower seed byproduct and its fractions for food application: an attempt to improve the sustainability of the oil process. *J. Food Sci.* **86**, 1497–1510 (2021).
3. Hladni, N. et al. Sunflower and abiotic stress: genetics and breeding for resistance in the -omics era sunflower abiotic stress breeding. In *Genomic Designing for Abiotic Stress Resistant Oilseed Crops* (ed Kole, C.) (Springer, 2022).
4. Puttha, R. et al. Charoenphun, N. Exploring the potential of sunflowers: agronomy, applications, and opportunities within bio-circular-green economy. *Horticulturae* **9**, 1079 (2023).
5. Beteri, J., Lyimo, J. G. & Msinde, J. V. The influence of climatic and environmental variables on sunflower planting season suitability in Tanzania. *Sci. Rep.* **14**, 3906 (2024).
6. Seiler, G. J., Qi, L. L. & Marek, L. F. Utilization of sunflower crop wild relatives for cultivated sunflower improvement. *Crop Sci.* **57**, 1083–1101 (2017).
7. Leclercq, P. Une stérilité cytoplasmique chez le tournesol. *Ann. De l'amélioration des. Plantes.* **19**, 99–106 (1969).
8. Kinman, M. L. New developments in the USDA and state experiment station sunflower breeding programs. In *Proceedings 4th International Sunflower Conference, Memphis, TN, USA* (1970).
9. De , E. et al. Sunflower seed production: Past, present, and perspectives. In *Proceedings of the 18th International Sunflower Conference, Mar del Plata, Argentina* (2012).
10. Toennissen, G. H. Feeding the world in the 21st century: Plant breeding, biotechnology and the potential role of apomixis. In *The Flowering of Apomixis: from Mechanisms to Genetic Engineering* (eds Savidan, Y. et al.) (CIMMYT, IRD, European Commission DG VI (FAIR), 2001).
11. Barcaccia, G. & Albertini, E. Apomixis in plant reproduction: a novel perspective on an old dilemma. *Plant. Reprod.* **26** (3), 159–179 (2013).
12. Xiong, J. et al. Synthetic apomixis: the beginning of a new era. *Curr. Opin. Biotechnol.* **79**, 102877 (2023).
13. Xiong, J. et al. Sexual reproduction vs unisexual; asexual reproduction, plants. *Encyclopedia of Reproduction*, (ed Skinner, M. K.) (Elsevier, 2018).
14. Hojsgaard, D. & Pullaiah, T. *Apomixis in Angiosperms: Mechanisms, Occurrences, and Biotechnology* 274 (CRC Press, 2022).
15. Acuña, C. A. et al. Reproductive systems in Paspalum: relevance for germplasm collection and conservation, breeding techniques, and adoption of released cultivars. *Front. Plant Sci.* **21**, 10, 1377 (2019).
16. Menéndez, A., Bianchi, M. B., Picardi, L. A., Nestares, G. M. & Ochogavía, A. C. Developmental variability in advanced megagametogenesis and embryogenesis in cultivars of sunflower (*Helianthus annuus* L.). *Crop Sci.* **62** (3), 31024–31036 (2022).
17. Voronova, O. Development of female reproduction structures and apomixis in some CMS lines of sunflower. *Helia* **36**, 47–60 (2013).
18. Hand, M. L. & Koltunow, A. M. G. The genetic control of apomixis: asexual seed formation. *Genetics* **197** (2), 441–450 (2014).
19. Hörndl, E. Apomixis and the paradox of sex in plants. *Ann. Botany* **134** (1), 1–18 (2024).
20. Bashaw, E. C., Hussey, M. A. & Hignight, K. W. Hybridization (N+N and 2 N+N) of facultative apomictic species in the *Pennisetum* agamic complex. *Int. J. Plant. Sci.* **153** (3), 466–470 (1992).
21. Martínez, E. J., Espinoza, F. & Quarín, C. L. BIII progeny (2n+n) from apomictic *Paspalum notatum* obtained through early pollination. *J. Hered.* **85**, 295–297 (1994).
22. Espinoza, F., Pessino, S. C., Quarín, C. L. & Valle, E. M. Effect of pollination timing on the rate of apomictic reproduction revealed by RAPD markers in *Paspalum notatum*. *Ann. Botany* **89**, 165–170 (2002).
23. Nogler, G. A. Genetics of gametophytic apomixis—a historical sketch. *Pol. Bot. Stud.* **8**, 5–11 (1994).
24. Nogler, G. A., Ozias-Akins, P. & Van Dijk, P. Mendelian genetics of apomixis in plants. *Annu. Rev. Genet.* **41**, 509–537 (2007).

25. Barke, H. B., Daubert, M. & Hörald, E. Establishment of Apomixis in Diploid F_2 hybrids and inheritance of apospory from F_1 to F_2 hybrids of the *Ranunculus auricomus* Complex. *Front. Plant. Sci.* **9**, 1111 (2018).
26. Schinkel, C. C. F. et al. Pathways to polyploidy: indications of a female triploid bridge in the alpine species *Ranunculus Kuepferi* (Ranunculaceae). *Plant Syst. Evol.* **303**, 1093–1108 (2017).
27. Ochogavia, A. C. Quantifying the reproductive progression of sunflower using FIJI (Image J). *MethodsX* **9**, 101879 (2022).
28. Schneiter, A. A. & Miller, J. F. Description of sunflower growth stages. *Crop Sci.* **21**, 901–903 (1981).
29. Marconi, G. et al. Methylation content sensitive enzyme ddRAD (MCSeEd): a reference-free, whole genome profiling system to address cytosine/adenine methylation changes. *Sci. Rep.* **9**, 14864 (2019).
30. Bashir, T. et al. Hybridization alters spontaneous mutation rates in a parent-of-origin-dependent fashion in *Arabidopsis*. *Plant Physiol.* **165**, 424–437 (2014).
31. Yang, S. et al. Parent-progeny sequencing indicates higher mutation rates in heterozygotes. *Nature* **523**, 463–467 (2015).
32. Xie, Z. et al. Mutation rate analysis via parent-progeny sequencing of the perennial peach. I. A low rate in woody perennials and a higher mutagenicity in hybrids. *Proc. R. Soc. B Biol. Sci.* **283** (2016).
33. Albertini, E., Barcaccia, G., Carman, J. G. & Pupilli, F. Did Apomixis evolve from sex or was it the other way around? *J. Exp. Bot.* **70**, 2951–2964 (2019).
34. Schmidt, A. Controlling apomixis: shared features and distinct characteristics of gene regulation. *Genes* **11**, 329 (2020).
35. Ortiz, J. P., Pupilli, F., Acuña, A., Leblanc, O. & Pessino, S. C. How to become an apomixis model: the multifaceted case of *Paspalum*. *Genes* **11** (9), 974 (2020).
36. Carballo, J. et al. Differentially methylated genes involved in reproduction and ploidy levels in recent diploidized and tetraploidized *Eragrostis curvula* genotypes. *Plant. Reprod.* **37** (2), 133–145 (2023).
37. Hojsgaard, D. & Hörandl, E. The rise of apomixis in natural plant populations. *Front. Plant Sci.* **10**, 358 (2019).
38. Ortiz, J. P. et al. Harnessing apomictic reproduction in grasses: what we have learned from *Paspalum*. *Ann. Botany* **112**, 767–787 (2013).
39. Haig, D. & Westoby, M. Parent-specific gene expression and the triploid endosperm. *Am. Nat.* **134**, 147–155 (1989).
40. Stebbins, G. L. in *Seeds, Seedlings, and the Origin of Angiosperms. Origin and Early Evolution of Angiosperms* 300–311 (eds Beck, C. B.) (Columbia University, 1976).
41. Scott, R. J., Spielman, M., Bailey, J. & Dickinson, H. G. Parent-of-origin effects on seed development in *Arabidopsis thaliana*. *Development* **125**, 3329–3341 (1998).
42. Doll, N. M. & Ingram, G. C. Embryo-endosperm interactions. *Annu. Rev. Plant Biol.* **73**, 293–321 (2022).
43. Mecchia, M. A. et al. Genome polymorphisms and gene differential expression in a ‘back-and-forth’ ploidy-altered series of weeping lovegrass (*Eragrostis curvula*). *J. Plant Physiol.* **164**, 1051–1061 (2007).
44. Weihmüller, E. et al. Genetic response of *Paspalum plicatulum* to genome duplication. *Genetica* **142**, 227–234 (2014).
45. R Development Core Team. *R: A Language and Environment for Statistical Computing*. Version 3.0.0. (R Found. Stat. Comput., 2013).
46. Otto, P. DAPI staining of fixed cells for high-resolution flow cytometry of nuclear DNA. *Methods Cell. Biol.* **33**, 105–110 (1990).
47. Kallamadi, P. & Mulpuri, S. Ploidy analysis of *Helianthus* species by flow cytometry and its use in hybridity confirmation. *Nucleus* **59**, 123–130 (2016).
48. FlowJo™ Software Version 10.8.1. Ashland (Dickinson and Company, 2021).
49. Lersten, N. R. & Curtis, J. D. Secretory reservoirs (ducts) of two kinds in giant ragweed (*Ambrosia trifida*; Asteraceae). *Am. J. Bot.* **75**, 1313–1323 (1988).
50. Herr, J. M. Jr. A new clearing-squash technique for the study of ovule development in angiosperms. *Am. J. Bot.* **58**, 785–790 (1971).
51. Breccia, G. et al. Immature embryo culture for early screening of imidazolinone resistance in sunflower. *Int. J. Plant. Breed.* **3**, 37–40 (2009).
52. Murashige, T. & Skoog, F. A revised medium for rapid growth and bio assays with tobacco tissue cultures. *Physiol. Plant.* **15** (3), 473–497 (1962).
53. Catchen, J., Hohenlohe, P. A., Bassham, S., Amores, A. & Cresko, W. A. Stacks: an analysis tool set for population genomics. *Mol. Ecol.* **22** (11), 3124–3140 (2013).
54. Purcell, S. et al. PLINK: a tool set for whole-genome association and population-based linkage analyses. *Am. J. Hum. Genet.* **81**, 559–575 (2007).

Acknowledgements

The authors would like to thank Dr. Julio González of the Instituto Nacional de Tecnología Agropecuaria (INTA) for seed materials.

Author contributions

SCP, GN, EA and ACO contributed to the conception and design of the study. Material preparation was performed by GN, IK, AL, and ACO. Cytoembryology analysis was conducted by SCP, MBB y ACO. The MCSeEd-based experiments were done by SCP, ACO, MB, GM and EA. GM and SCP analysed the MCSeEd data. ACO and SCP wrote the first draft of the manuscript. All authors revised and approved the final manuscript.

Funding

This research was funded by the European Union’s Horizon 2020 Research and Innovation Program under the Marie Skłodowska-Curie Grant Agreements 872417 (MAD) and 101007438 (POLYPLOID). Additionally, funding was received by the National Agency for the Promotion of Research, Technological Development and Innovation, Argentina (PICT 2021 – 539) and National University of Rosario, Argentina (PID 800 20220700266UR). SCP and ACO are research staff members of CONICET, Argentina.

Declarations

Competing interests

The authors declare no competing interests.

Additional information

Supplementary Information The online version contains supplementary material available at <https://doi.org/10.1038/s41598-025-89105-x>.

Correspondence and requests for materials should be addressed to A.C.O.

Reprints and permissions information is available at www.nature.com/reprints.

Publisher's note Springer Nature remains neutral with regard to jurisdictional claims in published maps and institutional affiliations.

Open Access This article is licensed under a Creative Commons Attribution-NonCommercial-NoDerivatives 4.0 International License, which permits any non-commercial use, sharing, distribution and reproduction in any medium or format, as long as you give appropriate credit to the original author(s) and the source, provide a link to the Creative Commons licence, and indicate if you modified the licensed material. You do not have permission under this licence to share adapted material derived from this article or parts of it. The images or other third party material in this article are included in the article's Creative Commons licence, unless indicated otherwise in a credit line to the material. If material is not included in the article's Creative Commons licence and your intended use is not permitted by statutory regulation or exceeds the permitted use, you will need to obtain permission directly from the copyright holder. To view a copy of this licence, visit <http://creativecommons.org/licenses/by-nc-nd/4.0/>.

© The Author(s) 2025